Transfer of Functional Ceramic Thin Films Using a Thermal Release Process

Guangbin Dou, Andrew S. Holmes, Eric M. Yeatman, Robert V. Wright, Paul B. Kirby, and Chunyan Yin*

Being ferroelectric, piezoelectric, and pyroelectric, lead zirconate titanate (PZT) is one of the most useful and prominent electroceramics and is commonly used as the transduction element of actuators and sensors in microelectromechanical systems (MEMS) and micro-optics[1–6] and in memory devices.[7,8] It is also being explored for new applications such as nanorods,[9] domain physics,[10] and nanodevices.[11,12] Transfer of PZT thin films can allow integration of such films on substrates that are incompatible with the requirements of film deposition. However, transfer of functional ceramic thin films has long been hampered by the difficulty of detaching the film from the growth substrate.[13,14] Here, we describe a transfer process for PZT films grown on Ti/Pt coated Si wafers, where the films are solder bonded onto a target substrate and lifted off in one step, using separation of the PZT–Pt interface by thermal stress. The transferred films show low mechanical damage, ferroelectric hysteresis with an "imprinted" polarization,[15] reduced permittivity, and improved loss tangent.

Generally PZT films are epitaxially grown on ordered metal seed layers, such as Ti/Pt layers deposited on Si wafers, and require high-temperature processing for crystallization and poling.[16] Therefore, the transfer of these films onto target substrates is important to enable them to be used in integrated structures that are not compatible with these materials or process steps, such as organic substrates. Several techniques have been reported for transfer of PZT films to make devices, involving wet etching,[17] dry etching,[18] mechanical grinding and etching,[13] or laser induced forward transfer (LIFT).[14] Wet etching can be used to pattern PZT films, but is not practical for the etching of some metal seed layers, such as Pt, which is normally removed by dry etching. In a typical transfer process, a metal-bumped PZT film is first bonded onto a target substrate and then a lift-off process is required to separate the patterned film from the growth wafer. The grinding and etching transfer method has the advantage of low electrode loss at high frequencies,[13] but the grinding is difficult to control and this process is not suitable for high-volume manufacturing. LIFT is a simple and easily controlled process, but damage to the PZT films by the laser ablation is unavoidable, and a plasma repair process is normally recommended.[14] In this study, a transfer process without dry etching, grinding, or LIFT is demonstrated. In the process, metal-bumped PZT films are bonded onto a target substrate by Sn/Au soldering and lifted off from the source substrate by the thermal stresses created in the films during soldering.

PZT thin films, with the composition $PbZr_{0.3}Ti_{0.7}O_3$, were prepared using a previously reported sol-gel process.[15,19] In this process, PZT films around 0.5 μm in thickness were deposited on Ti/Pt-coated, thermally oxidized Si wafers and these had the highly preferred (111) crystallographic orientation, which is a characteristic feature of this process. Then the PZT-coated wafers were patterned with multilayer metal (Cr/Cu/Ni/Au/Sn/Au) bumps, by the processes of sputter coating, lithography, and electroplating, in various shapes. Subsequently, the bumped wafers were diced into rectangular samples as shown in **Figure 1**a–c. In order to bond the bumped PZT films, Si target substrates coated with Cr/Au layers were prepared with the same size as the PZT-coated samples. The transfer process had three steps. First, a cleaned PZT sample was aligned to the target substrate as shown in Figure 1a. Then the sample was reflowed on a hotplate or in a rapid thermal annealing (RTA) chamber as shown in Figure 1b. For the thermal reflow, water soluble flux was painted on the samples if a hotplate was used, while Ar gas was used to protect the solder from oxidizing in the RTA. In the last step, the sample was removed from the hotplate when the temperature dropped below 100 °C. It was found that all the bumped films detach from the source substrate and are soldered onto the target substrate, as illustrated in Figure 1c. Figure 1d,e show hexagonal and square PZT films transferred using the hotplate; Figure 1f shows the largest rectangular film transferred in the RTA. To measure the electrical properties of the PZT samples, Cr/Au electrodes were evaporated onto the transferred hexagonal PZT films as shown in Figure 1d. It can be seen that there is still some flux residue left on the substrates, although 80 °C deionized (DI) water was used to clean the transferred samples, as suggested by the flux manufacturer (Figure 1d,e). In comparison, the Ar gas protected transfer in the RTA chamber was a cleaner process, as the transferred sample shows in Figure 1f.

Examination by energy dispersive X-ray analysis shows that the transferred film is separated from the Pt layer, and SEM

Dr. G. Dou, Prof. A. S. Holmes, Prof. E. M. Yeatman
Electrical and Electronic Engineering Department
Imperial College London
London SW7 2AZ, UK
E-mail: g.dou@imperial.ac.uk
R. V. Wright, Dr. P. B. Kirby
Materials Department
Cranfield University
Cranfield MK43 0AL, UK
Dr. C. Yin
School of Computing and Mathematical Sciences
University of Greenwich
London SE10 9LS, UK

10.1002/adma.201004391

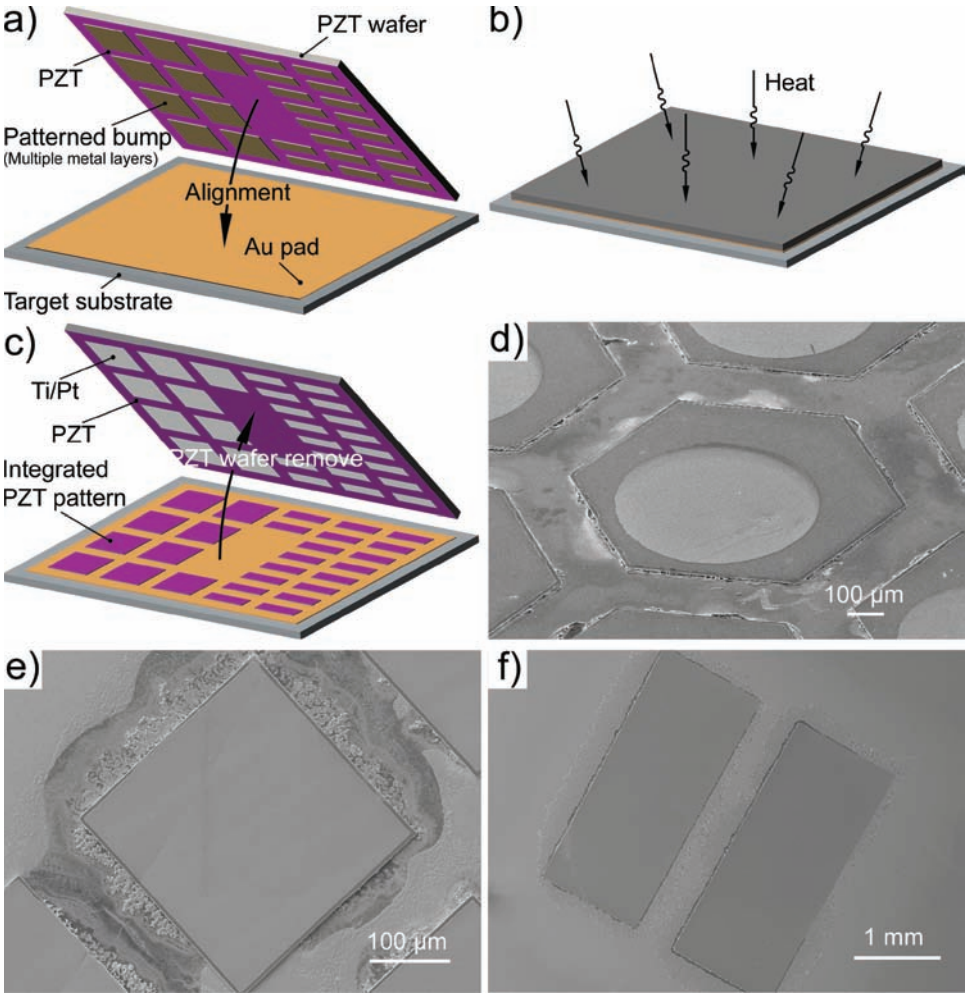

Figure 1. Schematic of solder transfer of PZT film including: a) alignment of source and target wafers, b) application of heat to reflow solder, and c) removal of source wafer. d) Scanning electron microscopy (SEM) image of a transferred hexagonal PZT film (1000 μm in longest diameter) with Cr/Au coated electrode (600 μm in diameter). e) SEM of a transferred square (600 μm × 600 μm). f) SEM image of a transferred rectangle, 3 mm × 1.25 mm, the largest one transferred in the process.

examination shows that the film is completely intact, with edges sharply defined by the solder bumped pattern, as shown in **Figure 2**a. The transferred film edge can be seen to be somewhat recessed from that of the solder bump. This is because the wet etching of the Cu/Cr seed layers undercuts the solder bump, and when the excess PZT breaks away during release it takes the pattern of the Cu/Cr to which it is directly bonded, rather than of the solder. Close up scanning electron microscopy (SEM) investigation shows there is no physical damage on the transferred PZT films (Figure 2b). SEM examination of the cross-section of the transferred samples shows that there is no damage in the interface between the PZT film and the Ni bump (Figure 2c) and the solder bonding is solid as shown in Figure 2d. To characterize the lift-off process further, PZT samples were reflowed without bonding onto a target substrate. Monitoring of this process showed that the lift-off process starts from one corner of the bumped PZT film at about 40 °C and extends quickly until the whole bumped area is lifted off. This lift-off process could be useful for making free-standing PZT films with multiple layer metal bumps, as shown in Figure 2e. Thermal stresses due to coefficient of thermal expansion (CTE) mismatch and stresses due to the solder solidification shrinkage are believed to be the main driving forces for the damage-free release of the film. To lift the film off, it requires the whole sample to go through a reflow process with a peak temperature of 320 °C. As the materials in the layered structure have different CTE, thermal stresses are built up in the sample when the temperature changes, particularly at the interfaces. Numerical modeling was used to study the lift-off of the free-standing films as detailed in Figure 2f,g. The results show that the periphery along the interface between the PZT film and the growth substrate exhibits high tensile stress when the temperature decreases (Figure 2f); higher shear stress was also identified at the corner area in this interface (Figure 2g). It should be noted that the modeling includes only linear thermal expansion, whereas in reality the solder will also shrink by 3–4% during solidification,[20,21] enhancing the effect due to thermal mismatch. The stresses produced will cause lifting

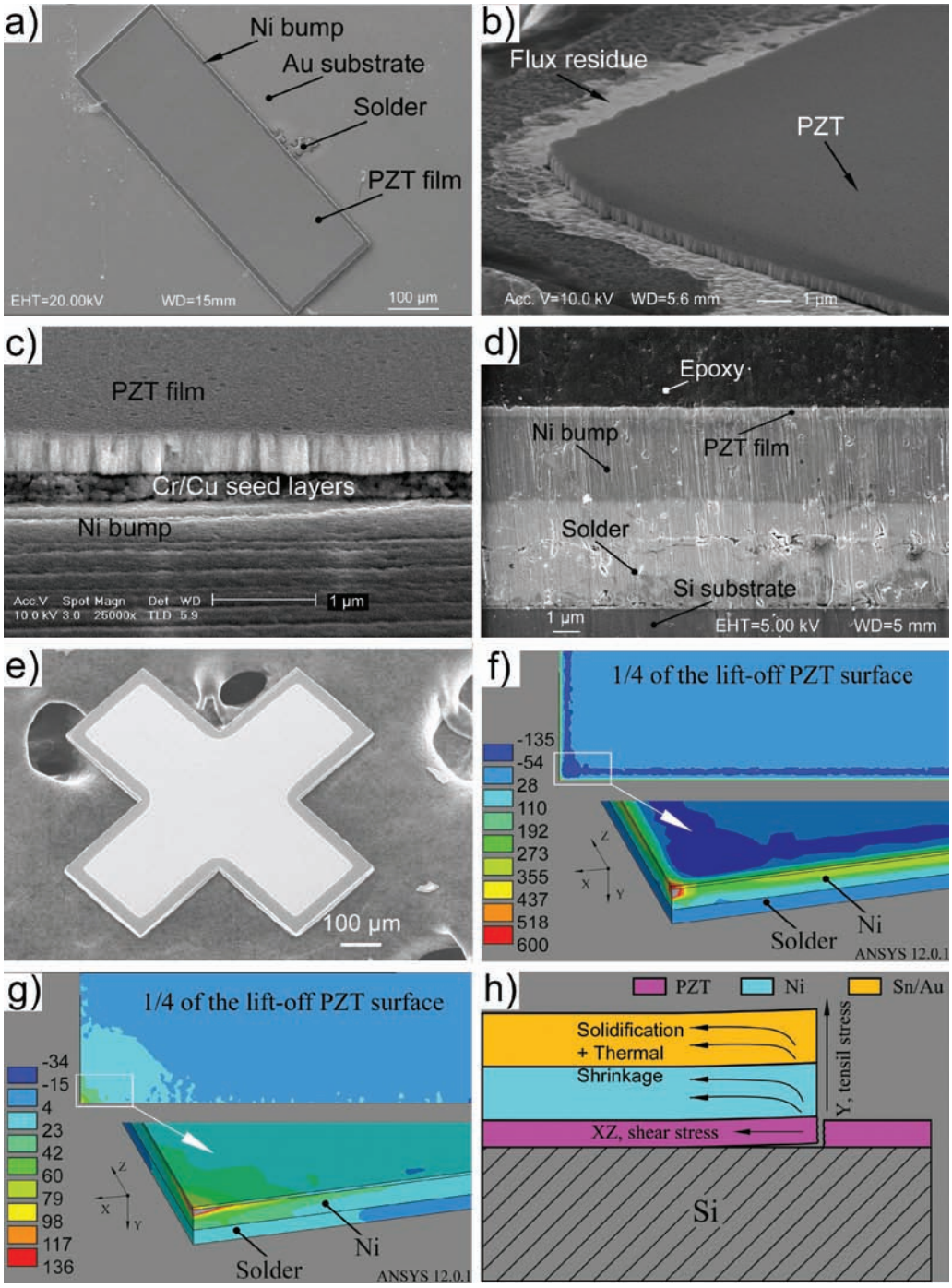

Figure 2. a) SEM image of a transferred rectangular PZT pattern, of size 600 µm × 200 µm. b) Close up SEM image of the transferred film. c) SEM image of an interface of the PZT film and Ni bump. d) SEM image of the solder joint cross-section. e) SEM image of a solder lifted, free-standing cross. f,g) Finite element method (FEM) analysis of the transfer mechanism (units: MPa): f) tensile (off line) stress, g) shear (in line) stress. ANSYS was employed to investigate the lift off of free-standing rectangular PZT patterns (600 µm × 200 µm). This work focused on modeling the thermally induced stress in the cooling down process from 280 °C to 25 °C. All the materials were assumed as stress free at 280 °C and elastic with temperature-independent CTE in the cooling process. One quarter of the geometry was modeled with appropriate boundary conditions on the symmetry surfaces. Seed layers were not considered as they are much thinner than the Ni and solder layers. h) Mechanisms of damage-free release.

off to occur when they exceed the adhesion forces at the interface. Combining the experimental and modeling results, the damage-free lift off process can be summarized as illustrated in Figure 2h. During the solder reflow, the solidification and thermal shrinkage cause tensile (off line) and shear (in line) stresses on the film, which produce separation along the PZT-Pt interface. Detachment of metal pads from organic substrates by a similar mechanism has been observed previously.[22,23]

Figure 3a–c show the electrical test results for the PZT samples, including polarization–electric field (*P*–*E*) hysteresis, dielectric constant, and loss tangent. These results were measured from the samples labeled AS, AB, and AT in the figures, corresponding, respectively, to as-deposited, after solder bumping, and after solder transfer. In Figure 3a, the *P*–*E* loops are single loops measured at a frequency of 100 Hz and indicate that the films before and after solder transfer are ferroelectric. The *P*–*E* loop (AS) measured from the sample as-deposited has symmetric coercivity (E_C = 100 kV cm^{-1}), but the positive remnant polarization (P_{r+} = +32 μC cm^{-2}) is slightly larger than the negative (P_{r-} = −26 μC cm^{-2}). This asymmetry may be due to the use of different bottom and top electrodes, Ti/Pt and Au/Cr, respectively.[16] Compared to the AS loop, the loop (AB) measured from the sample after solder bumping has smaller remnant polarization and asymmetric coercivity. The lower P_r could be caused by the stress in the PZT film induced by the electroplating of the multiple metal solder bump. The asymmetric coercivity shows that the PZT film is "imprinted"[16] with a shift such that $|P_{r+}| > |P_{r-}|$ and $|E_{c+}| < |E_{c-}|$ and this effect, which is more pronounced after film transfer (AT), indicates the presence of internal electric fields. If, as seems most likely, these are located at the PZT-electrode interfaces, and also considering that the effect is not seen with evaporated contacts (loop AS), we believe these are produced by defects introduced during the electrode sputtering process, either during sputter cleaning of the PZT surface or in the newly formed interface between the transferred film and the soldered electrode, and that the defects are redistributed, so enhancing the effect, following the thermal or mechanical film transfer processing. However, the remnant polarization of the imprinted AT loop is the highest among the three cases, a benefit of the solder transfer technique. The large polarization is likely to be contributed by the non-180° domains, which are pinned by the sol-gel induced stress but released in the solder transfer. This assumption is further supported by the increased coercive field observed for the AT loop, as it is expected that the non-180° domains would be harder to switch than the 180° domains.

Capacitance and loss (tanδ) of the PZT films before and after solder transfer were measured using a signal of 1 V at 1, 10, 100, 200, and 300 kHz. From the measured capacitance, the dielectric constant (k) of the parallel plate PZT capacitor can be calculated, as plotted in Figure. 3b. It shows that k is reduced as the signal frequency increases. The value for the film as sol-gel deposited (AS), at >420, is higher than for the films after solder bumping (AB) and transfer (AT), at <340. The reduced k for the AB and AT samples may be caused by damage and defects and the newly formed interface, as discussed above. It may also be an apparent reduction caused by the introduction of a very thin parasitic layer of low k, which is in series with the ferroelectric layer.[24] The k across multiple samples is more consistent after solder bumping and transfer, as indicated by the standard deviation bars in the figure. However, this may simply result from the more reliable contact of the sputter-coated electrodes of the transferred films, compared to the evaporation deposited electrodes used to characterize as-deposited films.

Figure 3c shows the measured loss tangent for samples before and after solder transfer. The values for AS samples are less than 3% for signal frequencies below 10 kHz, but increase sharply to more than 8% above 100 kHz. Similarly, the losses for AB samples increase with frequency, but their values are about half those of AS samples. In comparison, the losses in the solder transferred AT samples do not show this strong increase with frequency. This is likely to be caused by the presence of series resistance in the former samples, which will have the effect of an apparent increase with frequency of tan(δ). Compared to the Cr/Cu (50/200 nm) electrodes on the solder transferred samples, the thinner Pt/Ti (100/10 nm) electrodes on the as-deposited films have lower conductivity, forming a larger resistor in series with the parallel plate PZT capacitors. The release of the sol-gel stress in the transferred films may also contribute to the reduced loss.

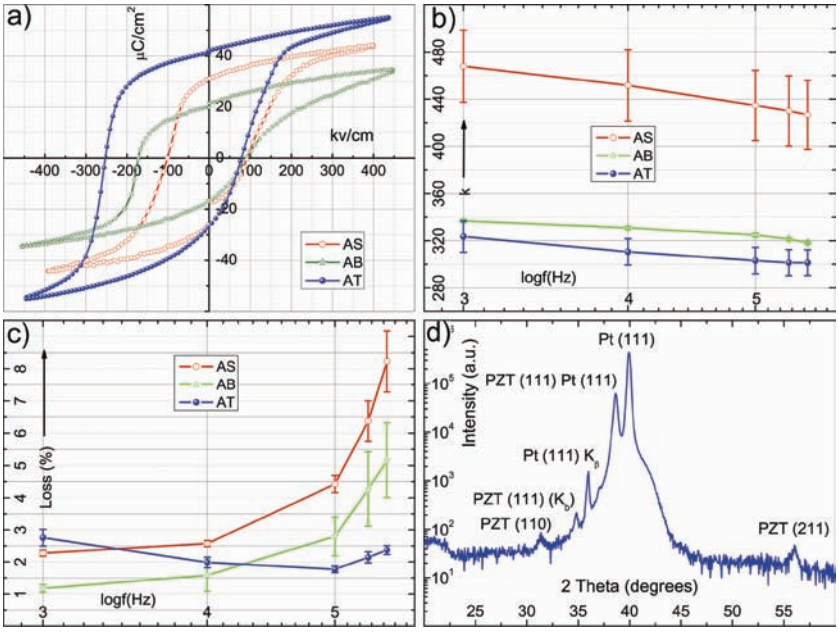

Figure 3. a–c) Electrical characterization of sol-gel deposited PZT film, as-deposited (AS), after solder bumping (AB), and after transfer (AT): a) *P*–*E* hysteresis loops, b) dielectric constant vs frequency, and c) loss tangent vs frequency. d) X-ray diffraction (XRD) pattern of sol-gel deposited PZT film.

In summary, we have introduced a transfer technique for functional ceramic thin films using a thermal release process. We believe that the release of the PZT film is driven by the stress induced by the large solidification shrinkage of the lead-free solder and CTE mismatch between the Si wafer (3.12 ppm per °C) and the Sn20Au80 alloy (16.2 ppm per °C) in the reflow.[20–23,25] The merit of this transfer process is that it allows bonding and lift-off of the thin films onto a target substrate in a single step. The solder-based PZT film transfer process reported here can be considered as a thin film printing technique, where the bumped area defines the PZT film pattern to be printed onto the target substrate.

The process induces no visible damage as shown in Figure 2b, and the transferred films are ferroelectric with slightly reduced dielectric constant and low loss tangent even at high frequency. However, the *P–E* loop of the transferred PZT film was found to be imprinted. The higher saturation polarization, which is advantageous for many device applications, is believed to be due to reduced clamping of the transferred film, enabling non-180° domains to participate in the polarization switching process. The shift along the field axis for the transferred film is believed to be mainly an electrode effect, as it is present to a lesser extent prior to the solder transfer. We conclude from these initial observations that PZT films are not significantly degraded during the transfer process, although detailed reliability tests are required to establish this more fully. This technique can be adapted to other thin film types that are compatible with the thermal solder bonding step.

Experimental Section

PZT Film Deposition: In the process, a sol-gel solution is spin-coated onto Ti/Pt (10/100 nm) coated, thermally oxidized Si wafers (ϕ 100 mm). Following spin-coating, the films are hotplate baked in air, first at 200 °C for 2 min for pyrolysis and then at 530 °C for 5 min for crystallization. The spun layers are relatively thin (≈80 nm) and so the process is repeated 6–7 times to provide films of thickness around 0.5 µm.

XRD Analysis: PZT as-deposited films were structurally characterized by X-ray diffraction (XRD) using a Siemens D5005 X-Ray Diffractometer configured for CuK_{α} radiation. As can be seen in the θ–2θ XRD trace of Figure 3d full crystallization of the perovskite phase has been achieved, indicated by the presence of (110), (111), and (211) peaks, with no evidence of the parasitic pyrochlore phase, which has its main 2θ peak at ≈30. Additional observed peaks are due to a low level of unfiltered CuK_{β} in the source.

Microscopy: The transferred PZT patterns were imaged and studied by scanning electron microscopy (SEM, LEO 1450VP) with energy dispersive X-ray (EDX) function. The solder joints were imaged by SEM (LEO 1530VP Field Emission Gun SEM) after sputtering with a thin Au layer.

Preparation of Transfer Samples: PZT-coated wafers were first sputter coated with Cu/Cr (50/200 nm) seed layers, then photoresist (AZ9260) was coated and patterned with hexagonal (1000 µm in longest diameter), square (600 µm by 600 µm) and rectangular (600 µm by 200 µm) apertures. Next multilayer metal bumps were electroplated in the apertures, comprising a Ni (2 µm) barrier layer and Au/Sn/Au (0.25/1.2/0.25 µm) solder layers. Subsequently, the photoresist was stripped off and the uncoated seed layers were removed by wet etching. The wafers were then diced into rectangular samples (9.4 mm by 7.8 mm) as shown in Figure 1a.

Target Substrate Preparation: In order to bond the bumped PZT films, Si target substrates coated with Cr/Au (50/250 nm) layers were prepared with the same size as the PZT-coated samples.

Thin Film Transfer: Hotplate (CAT MSC 66) and RTA (AG Associates Heatpulse 410) were used in this study for thermal reflow. Before the reflow, PZT samples were cleaned in acetone and DI water and painted with water soluble flux if the hotplate was used, or Ar gas protection was adopted in the RTA chamber. In the Sn20/Au80 reflow, the maximum temperature is 320 °C and the dwell time over 280 °C is 60 s.

Electrical Test Samples: To measure the electrical properties of the PZT samples, Cr/Au (10/100 nm) electrodes were evaporated onto the transferred PZT films through Si shadow masks.

Electrical Measurements: Capacitance and loss of PZT films before and after solder transfer were measured by a Wayne-Kerr 6425 Precision Component Analyzer. The *P–E* loops were measured by a Radiant Technologies RT66a Ferroelectric Test System.

Acknowledgements

This work is supported by the Engineering and Physical Sciences Research Council through the project Integrated Functional Materials for System-in-Package Applications.The authors would like to thank Dr. Qi Zhang at Cranfield University and Prof. Chunqing Wang at Harbin Institute of Technology for valuable discussions on the experimental results, as well as Mr. David Whalley for support on some of the reflow tests and Mr. Yi Qin for the preparation of the SEM cross-section at Loughborough University.

Received: November 29, 2010
Published online:

[1] I. Kanno, S. Fujii, T. Kamada, R. Takayama, *Appl. Phys. Lett.* **1997**, *70*, 1378.
[2] C.-K. Kao, C.-H. Tsaia, *Appl. Phys. Lett.* **2003**, *83*, 3915.
[3] S. H. Pu, A. S. Holmes, E. M. Yeatman, C. Papavassiliou, S. Lucyszyn, *J. Micromech. Microeng.* **2010**, *20*, 035030.
[4] J. Ma, Z. Shi, C.-W. Nan, *Adv. Mater.* **2007**, *19*, 2571.
[5] W. Eerenstein, N. D. Mathur, J. F. Scott, *Nature* **2006**, *442*, 759.
[6] H. Zheng, F. Straub, Q. Zhan, P. Yang, W. Hsieh, F. Zavaliche, Y. Chu, U. Dahmen, R. Ramesh, *Adv. Mater.* **2006**, *18*, 2747.
[7] A. Q. Jiang, H. J. Lee, G. H. Kim, C. S. Hwang, *Adv. Mater.* **2009**, *21*, 2870.
[8] B. Lei, C. Li, D. Zhang, Q. F. Zhou, K. K. Shung, C. Zhou, *Appl. Phys. Lett.* **2004**, *84*, 4553.
[9] S. J. Limmer, S. Seraji, M. J. Forbess, Y. Wu, T. P. Chou, C. Nguyen, G. Cao, *Adv. Mater.* **2001**, *13*, 1269.
[10] S. Bühlmann, P. Muralt, *Adv. Mater.* **2008**, *20*, 3090.
[11] R. F. Service, *Science* **2010**, *328*, 304.
[12] L. Tattini, P. Lo Nostro, A. Ravalli, M. Stirner, P. Baglioni, *J. Nanopart. Res.* DOI: 10.1007/s11051–010-9930–5.
[13] T. Riekkinen, T. Mattila, S. van Dijkena, A. Lüker, Q. Zhang, P. B. Kirby, A. M. Sánchez, *Appl. Phys. Lett.* **2007**, *91*, 252902.
[14] L. Tsakalakos, T. Sands, *Appl. Phys. Lett.* **2000**, *76*, 227.
[15] J. Lee, C. H. Choi, B. H. Park, T. W. Noh, *Appl. Phys. Lett.* **1998**, *72*, 3380.
[16] Q. Zhang, R. W. Whatmore, *J. Phys. D: Appl. Phys.* **2001**, *34*, 2296.
[17] K. Zheng, J. Lu, J. Chu, *Jpn. J. Appl. Phys.* **2004**, *43*, 3934.
[18] Y. Kokaze, I. Kimura, M. Endo, M. Ueda, S. Kikuchi, Y. Nishioka, K. Suu, *Jpn. J. Appl. Phys.* **2007**, *46*, 280.
[19] Q. Zhang, R. W. Whatmore, *Integr. Ferroelectr.* **2001**, *41*, 43.
[20] N. Sobczak, A. Kudyba, R. Nowak, W. Radziwill, K. Pietrzak, *Pure Appl. Chem.* **2007**, *79*, 1755.
[21] S. Belyakov, H. V. Atkinson, S. P. A. Gill, *J. Electric Mater.* **2001**, *39*, 1295.
[22] K. Suganuma, *Scripta Mater.* **1998**, *38*, 1333.
[23] K. Suganuma, M. Ueshima, I. Ohnak, H. Yasuda, J. Zhu, T. Matsuda, *Acta Mater.* **2000**, *48*, 4475.
[24] A. Q. Jiang, Y. Y. Lin, T. A. Tang, *J. Appl. Phys.* **2007**, *101*, 056103.
[25] K. Hungar, W. Mokwa, *J. Micromech. Microeng.* **2008**, *18*, 064002.